



# Orthogonal experimental study on unconfined compressive strength of a novel flow filling material

Yanpeng Zhu\*, Tao Huang<sup>a</sup>, Anping Huang<sup>b</sup>, Dong Chen<sup>c</sup>, Linping Wu<sup>d</sup>

Lanzhou University of Technology, Lanzhou, 730050, China

\*zhuyp@lut.cn, <sup>a</sup>2510914637@qq.com, <sup>b</sup>huanganping1995@163.com  
<sup>c</sup>ddong1996@163.com, <sup>d</sup>wlping@163.com

**Abstract.** A certain project in Lanzhou generated a large amount of abandoned collapsible loess and red sandstone during the excavation process. In order to achieve the dual goals of saving construction resources and protecting the environment, a certain proportion of cement, fly ash, lime, and NaOH are added to solidify and improve the abandoned soil, and it is prepared into a fluid filling material. Through orthogonal design, unconfined compressive strength tests are conducted on fluidic solidified soil with different ratios. The influencing factors and their significance are analyzed, the optimal proportions of each factor are obtained, and the regression equation of unconfined compressive strength is formulated. Additionally, the microstructure of the soil is studied. The results show that the cement content has the most significant impact on the unconfined compressive strength, followed by the fly ash content. The order of the influence of all factors on the unconfined compressive strength is as follows: cement content > fly ash content > mass ratio of collapsible loess to red sandstone > NaOH content > lime content. The amount of soil voids and cementitious materials determines the magnitude of compressive strength. The research results provide certain references for the preparation of fluidic solidified soil in collapsible loess and red sandstone areas.

**Keywords:** Construction resources; Solidification improvement; Construction technique; Orthogonal experiment; Collapsible loess; red sandstone; Underground engineering.

## 1 Introduction

At present, common backfilling projects mainly include the backfilling of foundation pits and fertilizer tanks, the backfilling of comprehensive pipe galleries, and the backfilling of underground pipe networks<sup>[1]</sup>. These types of projects are often carried out after the completion of the main structure construction. Due to the narrow construction surface and difficulty in compacting the support structure below, traditional backfilling techniques are difficult to meet the compactness requirements of backfill soil<sup>[2]</sup>. Insufficiently compacted backfill soil may experience excessive compaction settlement and collapsibility compression at a later stage, leading to potential structural damage to the

© The Author(s) 2024

P. Liu et al. (eds.), *Proceedings of the 2024 5th International Conference on Civil, Architecture and Disaster Prevention and Control (CADPC 2024)*, Atlantis Highlights in Engineering 31,

[https://doi.org/10.2991/978-94-6463-435-8\\_10](https://doi.org/10.2991/978-94-6463-435-8_10)

building. Therefore, addressing trench backfilling under narrow and irregular working surfaces has become an urgent priority.

Fluidic solidified soil is a self-compacting and self-leveling filling material<sup>[3]</sup>. It can not only address the challenge of trench backfilling under narrow and irregular working surfaces but also reuse the waste soil generated during the construction process, contributing to energy conservation and emission reduction. Since the introduction of fluidic solidified soil, it has been widely studied by scholars worldwide<sup>[4-7]</sup>. Liu et al.<sup>[8]</sup> applied the premixed fluidic solidified soil technology to the backfilling project of the underground comprehensive pipe gallery foundation and proposed a new method for the backfilling of the pipeline galleries. In order to use the waste soil generated by excavation in fill engineering, Chen et al.<sup>[9]</sup> studied the influences of cement and fly ash content and age on the unconfined compressive strength of fluidic solidified soil, using the silty clay, cement, and fly ash generated during excavation as raw materials. Wang et al.<sup>[10]</sup> used waste soil and cement excavated by the Zhengzhou subway as raw materials to study the failure mode of fluidic solidified soil while considering fluidity and compressive strength. Guo et al.<sup>[11]</sup> conducted a comparative analysis of the strength, fluidity, and water stability between common engineering soil and construction waste soil. Their research demonstrated that construction waste soil also exhibits excellent fluidic solidification performance. Wang et al.<sup>[12]</sup> prepared fluidic solidified soil using cement, steel slag powder, and industrial solid waste red mud. This approach improved the mechanical properties of fluidic solidified soil, reduced the amount of cement used, and explained the solidification mechanism of fluidic solidified soil from a microscopic perspective. Although the aforementioned scholars have conducted in-depth research on the influencing factors and properties of fluidic solidified soil, there is a lack of research on fluidic solidified soil with collapsible loess and red sandstone as aggregates under alkali excitation. If the research discovers that collapsible loess and red sandstone can be prepared into a composite fluidic solidified soil that meets the required specifications, this not only promotes the reuse and resource utilization of engineering waste soil but also contributes to the development of new materials that cater to various engineering needs, thereby driving innovation and development in this technological field.

As a type of remolded soil, the compressive strength of fluidic solidified soil is one of the important indicators to evaluate its soil performance, and it is an important basis for judging whether it can be applied to engineering. In this paper, waste collapsible loess and red sandstone produced after the excavation of a project in Lanzhou are used as aggregates, combined with cement, fly ash, lime, and NaOH to prepare fluidic solidified soil. Under the premise of ensuring fluidity, the influence of the mass ratio of collapsible loess to red sandstone, cement, fly ash, lime, and NaOH content on the unconfined compressive strength of fluidic solidified soil is quantitatively analyzed through orthogonal experiments. Moreover, the causes of the strength formation of fluidic solidified soil are studied from the microscopic level, which provides a theoretical basis for the application of fluidic solidified soil in collapsible loess and red sandstone areas in northwest China.

## 2 Materials and Experimental Methodology

### 2.1 Materials

The collapsible loess and red sandstone used in the experiment are waste soil generated during the excavation process of a project in Lanzhou. The collapsible loess was treated with a 2 mm sieve to remove impurities as fine aggregate, and the red sandstone was crushed with a crusher, passing through 2 mm and 5 mm sieves respectively. Particles with a particle size of 2-5 mm were taken as coarse aggregates. Figure 1 shows the particle size distribution diagram of collapsible loess, and Figures 2a and 2b show the XRD results of collapsible loess and red sandstone. The cement used in the experiment is P.O 42.5 ordinary Portland cement, the fly ash is a grade I fly ash, the lime has a CaO content of 95%, NaOH purity of 98%, and the water is local tap water from Lanzhou. The addition of cement effectively enhances the compressive strength of fluidic solidified soil and shortens its initial setting time. At the same time, the introduction of fly ash not only helps improve the fluidity of fluidic solidified soil and reduce shrinkage but also actively responds to environmental protection concepts. In addition, the addition of lime supplements the required  $\text{Ca}^{2+}$  for the hydration process, while NaOH further stimulates the activity of fly ash, collectively enhancing the performance of fluidic solidified soil. The physical properties and chemical composition of the experimental materials are shown in Tables 1-5.

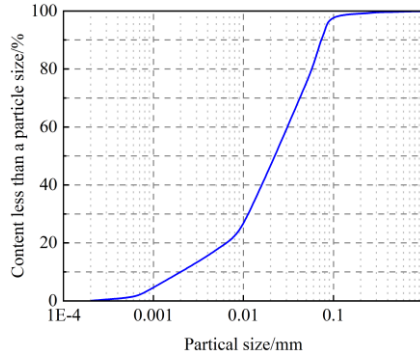
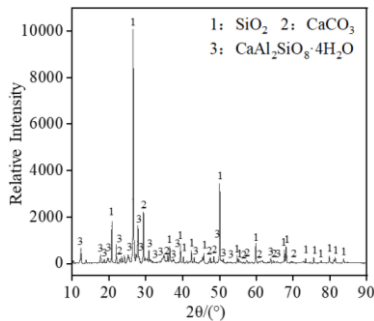
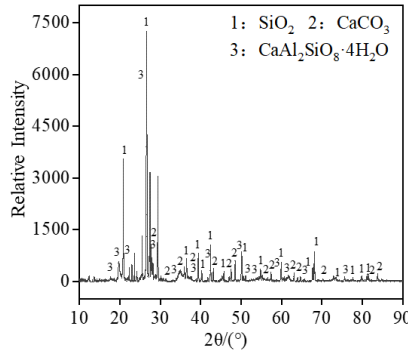


**Fig. 1.** Particle size distribution diagram of collapsible loess



(a) XRD results of collapsible loess



(b) XRD results of red sandstone

**Fig. 2.** XRD results

**Table 1.** Basic physical properties of collapsible loess used in the experiment

Natural Moisture Content/%	Liquid Limit/%	Plastic Limit/%	Plastic Limit Index	Liquid Limit Index
7.98	25.19	16.43	8.85	0.12

**Table 2.** Basic physical properties of red sandstone used in the experiment

Natural Density/(g.cm <sup>-3</sup> )	Specific Gravity	Void Ratio	Cohesive Force/kPa	Internal Friction Angle /°
1.75	2.60	1.42	23.10	32.35

**Table 3.** Chemical composition of cement and fly ash

Chemical Composition	CaO	Al <sub>2</sub> O <sub>3</sub>	SiO <sub>2</sub>	Fe <sub>2</sub> O <sub>3</sub>	Other
cement/%	62.87	4.49	23.15	2.84	4.63
Fly Ash/%	2.66	32.79	56.36	4.43	4.41

**Table 4.** Chemical composition of lime

Chemical Composition	CaO	Saltness	Alkali Metal	Loss on Ignition	Other
Percentage	95.7	0.25	0.37	3.2	0.42

**Table 5.** Chemical composition of NaOH

Chemical Composition	NaOH	Carbonate	Alkali Metal	Other
Percentage	98.6	0.20	0.11	0.15

## 2.2 Orthogonal Experimental Design

To investigate the impact of various factors on the unconfined compressive strength of fluidic solidified soil, the orthogonal experimental design is conducted to plan experiments. Five examination factors are considered: Factor A represents the mass ratio of collapsible loess and red sandstone, Factor B stands for the cement content, Factor C is the fly ash content, Factor D denotes the lime content, and Factor E is the NaOH content. The content of cement and fly ash is the percentage of each material to the mass of aggregate, and the content of lime and NaOH is the percentage of each material to the mass of fly ash. Five levels are selected for each factor, and an L25(5<sup>5</sup>) orthogonal table is used. The mix ratio of the orthogonal experimental scheme is shown in Table 6.

**Table 6.** Mix ratio of the orthogonal experimental scheme

Level	Factor A	Factor B/%	Factor C/%	Factor D/%	Factor E/%
1	80:20	4	3	0	0
2	75:25	5	6	4	2
3	70:30	6	9	8	4
4	65:35	7	12	12	6
5	60:40	8	15	16	8

## 2.3 Sample Preparation and Experimental Methods

During the sample preparation process, the lime and NaOH were dissolved in the pre-weighed water and then poured into a well-mixed material of collapsible loess, red sandstone, and fly ash, which were thoroughly stirred. In order to ensure the fluidity of the fluidic solidified soil, a cylindrical acrylic cylinder with an inner diameter and height of 80 mm was used for the test. According to the pre-test, water was continuously added in increments of 0.01 from a water solid ratio of 0.37 until the target flowability was not less than 160 mm<sup>[13]</sup>. The flowability test is shown in Figure 3.

According to the "Specification for Mix Proportion Design of Cement Soil" (JGJ T233-2011)<sup>[14]</sup>, a 70.7 mm x 70.7 mm x 70.7 mm cube mold was selected for the unconfined compressive strength test. After the sample was demoulded, it was maintained under the standard curing conditions with a humidity of over 95% and a temperature of 20 ± 2 °C. The curing period was set at 3, 7, 14, and 28 days. Three samples were prepared for each age under the same mix proportion, and the average value of the test results was taken. When the age was reached, the universal experimental press was used for the test, and the press speed was controlled to 1 mm/min until the sample was destroyed. The morphology of the damaged sample is shown in Figure 4.



**Fig. 3.** Liquidity test



**Fig. 4.** Morphology of the sample after destruction

### **3 Analysis of Experimental Results**

#### **3.1 Analysis of Orthogonal Experimental Results**

In this paper, the 28-day unconfined compressive strength was taken as an indicator. Firstly, the experimental results were visually analyzed using the intuitive analysis method. Then, the experimental data was processed using range analysis and variance analysis methods to determine the significance of the influence of the five factors on the experimental indicators and their impact rules on different indicators. The experimental data results are shown in Table 7.

##### **3.1.1 Intuitive Analysis**

As shown in Table 7, the unconfined compressive strength of samples in group 18 is the highest among all tests. At this time, the mass ratio of collapsible loess to red sandstone is 65:35, the content of cement is 6%, the content of fly ash is 15%, the content of lime is 8%, and the content of NaOH is 4%. The combination of fluidic solidified soil with the maximum unconfined compressive strength is  $A_4B_3C_5D_3E_3$ . It

shows that the combination of cement, fly ash, lime, and NaOH can significantly improve the unconfined compressive strength of fluidic solidified soil.

**Table 7.** Results of orthogonal experiments

No	Factor A	Factor	Factor	Factor	Factor	Unconfined Compression
		B/%	C/%	D/%	E/%	Strength /MPa
1	A <sub>1</sub>	B <sub>1</sub>	C <sub>1</sub>	D <sub>1</sub>	E <sub>1</sub>	0.55
2	A <sub>1</sub>	B <sub>2</sub>	C <sub>5</sub>	D <sub>4</sub>	E <sub>5</sub>	1.19
3	A <sub>1</sub>	B <sub>3</sub>	C <sub>4</sub>	D <sub>2</sub>	E <sub>4</sub>	1.31
4	A <sub>1</sub>	B <sub>4</sub>	C <sub>3</sub>	D <sub>5</sub>	E <sub>3</sub>	1.59
5	A <sub>1</sub>	B <sub>5</sub>	C <sub>2</sub>	D <sub>3</sub>	E <sub>2</sub>	1.65
6	A <sub>2</sub>	B <sub>1</sub>	C <sub>3</sub>	D <sub>3</sub>	E <sub>4</sub>	0.83
7	A <sub>2</sub>	B <sub>2</sub>	C <sub>2</sub>	D <sub>1</sub>	E <sub>3</sub>	1.00
8	A <sub>2</sub>	B <sub>3</sub>	C <sub>1</sub>	D <sub>4</sub>	E <sub>2</sub>	1.09
9	A <sub>2</sub>	B <sub>4</sub>	C <sub>5</sub>	D <sub>2</sub>	E <sub>1</sub>	1.71
10	A <sub>2</sub>	B <sub>5</sub>	C <sub>4</sub>	D <sub>5</sub>	E <sub>5</sub>	1.87
11	A <sub>3</sub>	B <sub>1</sub>	C <sub>5</sub>	D <sub>5</sub>	E <sub>2</sub>	1.20
12	A <sub>3</sub>	B <sub>2</sub>	C <sub>4</sub>	D <sub>3</sub>	E <sub>1</sub>	1.21
13	A <sub>3</sub>	B <sub>3</sub>	C <sub>3</sub>	D <sub>1</sub>	E <sub>5</sub>	1.28
14	A <sub>3</sub>	B <sub>4</sub>	C <sub>2</sub>	D <sub>4</sub>	E <sub>4</sub>	1.64
15	A <sub>3</sub>	B <sub>5</sub>	C <sub>1</sub>	D <sub>2</sub>	E <sub>3</sub>	1.67
16	A <sub>4</sub>	B <sub>1</sub>	C <sub>2</sub>	D <sub>2</sub>	E <sub>5</sub>	0.88
17	A <sub>4</sub>	B <sub>2</sub>	C <sub>1</sub>	D <sub>5</sub>	E <sub>4</sub>	1.22
18	A <sub>4</sub>	B <sub>3</sub>	C <sub>5</sub>	D <sub>3</sub>	E <sub>3</sub>	2.28
19	A <sub>4</sub>	B <sub>4</sub>	C <sub>4</sub>	D <sub>1</sub>	E <sub>2</sub>	1.94
20	A <sub>4</sub>	B <sub>5</sub>	C <sub>3</sub>	D <sub>4</sub>	E <sub>1</sub>	2.08
21	A <sub>5</sub>	B <sub>1</sub>	C <sub>4</sub>	D <sub>4</sub>	E <sub>3</sub>	1.26
22	A <sub>5</sub>	B <sub>2</sub>	C <sub>3</sub>	D <sub>2</sub>	E <sub>2</sub>	1.49
23	A <sub>5</sub>	B <sub>3</sub>	C <sub>2</sub>	D <sub>5</sub>	E <sub>1</sub>	1.50
24	A <sub>5</sub>	B <sub>4</sub>	C <sub>1</sub>	D <sub>3</sub>	E <sub>5</sub>	1.23
25	A <sub>5</sub>	B <sub>5</sub>	C <sub>5</sub>	D <sub>1</sub>	E <sub>4</sub>	1.59

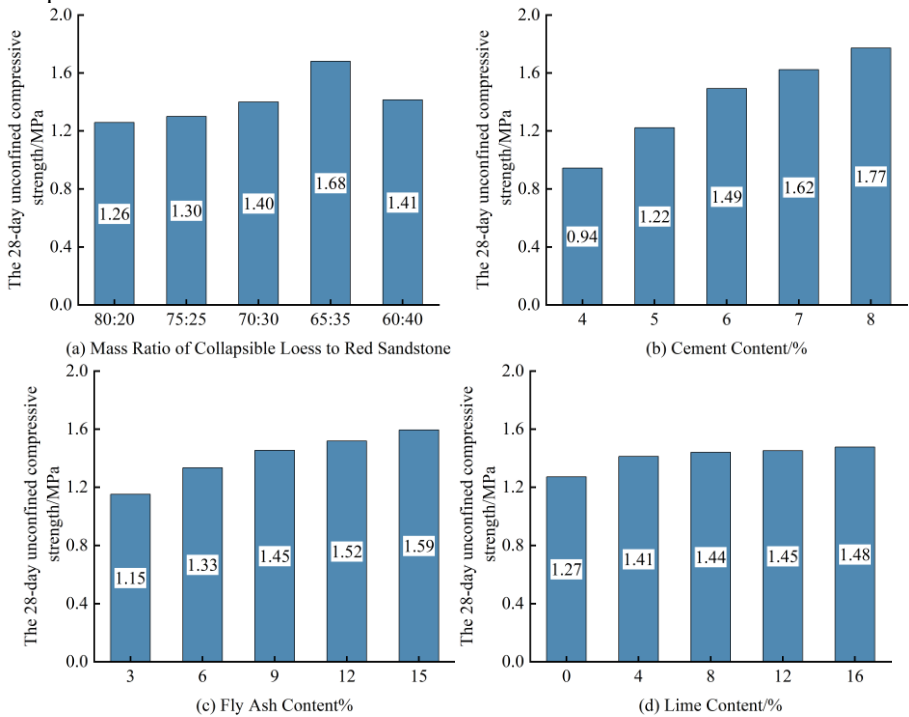
### 3.1.2 Range Analysis

In order to determine the order of the influence of different factors on the unconfined compressive strength, range analysis was conducted on the test results, as shown in Table 8.

**Table 8.** Range analysis results of orthogonal experiments

$K_i$ value	Factor A	Factor B/%	Factor C/%	Factor D/%	Factor E/%
$K_1$	6.29	4.72	5.76	6.36	7.05
$K_2$	6.50	6.11	6.67	7.06	7.37
$K_3$	7.00	7.46	7.27	7.20	7.80
$K_4$	8.40	8.11	7.59	7.26	6.59
$K_5$	7.07	8.86	7.97	7.38	6.45
$\bar{K}_1$	1.26	0.94	1.15	1.27	1.41
$\bar{K}_2$	1.30	1.22	1.33	1.41	1.47
$\bar{K}_3$	1.40	1.49	1.45	1.44	1.56
$\bar{K}_4$	1.68	1.62	1.52	1.45	1.32
$\bar{K}_5$	1.41	1.77	1.59	1.48	1.29
$R$	2.11	4.14	2.21	1.02	1.35

As shown in Table 8, the order of the influence of all factors on the unconfined compressive strength is as follows: cement content > fly ash content > mass ratio of collapsible loess to red sandstone > NaOH content > lime content.



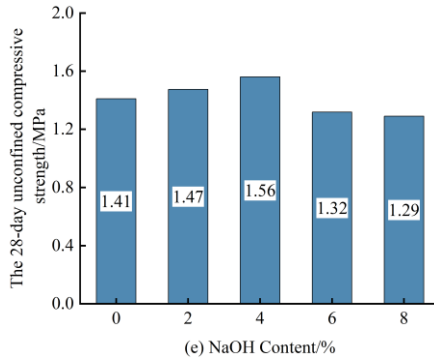


**Fig. 5.** Relationship between each factor and unconfined compressive strength

After orthogonal experimental analysis, the average unconfined compressive strength of each factor at each level can be calculated. The relationship between each factor and the unconfined compressive strength is shown in Figure 5.

As illustrated in Figure 5a, when factor A (mass ratio of collapsible loess to red sandstone) decreases, the unconfined compressive strength increases first and then decreases. At  $A_4$  (65:35), it shows a maximum value of 1.68 MPa, which is 0.42, 0.38, 0.28, and 0.27 MPa higher than  $A_1$ ,  $A_2$ ,  $A_3$ , and  $A_5$ , respectively. It can also be seen that the influence of factor A on the unconfined compressive strength from large to small is  $A_4 > A_5 > A_3 > A_2 > A_1$ . The above situation is because when the ratio of collapsible loess to red sandstone is 65:35, there is a large packing density and a small porosity, which can not only increase the compactness of the fluidic solidified soil but also reduce the amount of cementitious materials and the water solid ratio, thereby improving the unconfined compressive strength of the fluidic solidified soil.

Figures 5b and 5c show that the unconfined compressive strength increases with the increase of cement and fly ash content, but the influence of cement content on the unconfined compressive strength is more significant than that of fly ash. When the cement content increases from 4% to 8% and the fly ash content increases from 3% to 15%, the unconfined compressive strength of fluidic solidified soil increases by 87.7% and 38.4%, respectively. This is because the voids in the soil are filled with cementitious substances generated by cement hydration. A higher cement content results in increased generation of cementitious substances through hydration, leading to a greater degree of filling and higher macroscopic unconfined compressive strength exhibited by the fluidic solidified soil.

As shown in Figure 5d, with the increase of lime content, the unconfined compressive strength shows an increasing trend. When the lime content increases from 0% to 4%, the unconfined compressive strength increases by 11%. When the lime content increases from 4% to 16%, the unconfined compressive strength value only increases by 4.5%. This is due to the ion exchange effect in the mixing process of fluidic solidified soil. Calcium hydroxide (CH) produced by cement hydration is absorbed by the soil sample, so that the concentration of CH in the fluidic stabilized soil can not reach the saturation state, and the content of  $Ca^{2+}$  and  $OH^-$  required to produce the hydrated calcium silicate gel (C-S-H) decreases, resulting in the reduction of the production of

C-S-H, thus reducing the unconfined compressive strength of the fluidic stabilized soil. The addition of lime supplemented the missing  $\text{Ca}^{2+}$  and  $\text{OH}^-$ , which improved the unconfined compressive strength. However, when the lime content exceeded 4%, the  $\text{Ca}^{2+}$  and  $\text{OH}^-$  used to produce C-S-H in the fluidic solidified soil had reached saturation state. Therefore, the addition of more lime did not significantly improve the unconfined compressive strength.

As shown in Figure 5e, the unconfined compressive strength of fluidic solidified soil firstly increases and then decreases with the increase of the content of NaOH. When the NaOH content increases from 0% to 4%, the unconfined compressive strength gradually increases and reaches the maximum value of 1.56 MPa at 4% content. When the NaOH content increases from 4% to 8%, the unconfined compressive strength begins to decrease. This is because adding a small amount of NaOH can stimulate the activity of fly ash to generate more calcium aluminate hydrate (C-A-H) and aluminate silicosilicate (CA-S-H), which macroscopically shows an improvement in unconfined compressive strength. When the content of NaOH exceeds the optimal content, the soil structure of the fluidic solidified soil begins to be destroyed by NaOH, and the unconfined compressive strength shows a decreasing trend.

### 3.1.3 Analysis of Variance

Although range analysis can intuitively show the order of the influence of each factor on the unconfined compressive strength, it does not accurately analyze the errors of each factor, nor can it show the significance of the influence of each factor on the unconfined compressive strength. In order to compensate for the shortcomings of range analysis and adopt a more reliable analysis of variance, this article used IBM SPSS Statistics 27 software to conduct an analysis of variance on various factors. The analysis results are shown in Table 9.

**Table 9.** Analysis of variance

Factor	DEVSQ	Degree of Freedom	Mean Square	F Value	Significance
A	0.532	4	0.133	2.029	0.255
B	2.012	4	0.503	7.680	0.037
C	0.627	4	0.157	2.393	0.209
D	0.160	4	0.040	0.612	0.677
E	0.238	4	0.060	0.910	0.535
Error	0.262	4	0.065		
Sum	53.647	25			

According to Table 9, the order of the significance of unconfined compressive strength of fluidic solidified soil with collapsible loess and red sandstone as aggregates is as follows: cement content > fly ash content > mass ratio of collapsible loess to red sandstone > NaOH content > lime content. This is consistent with the conclusion obtained from the range analysis.

As depicted in Figure 5, all the unconfined compressive strengths of different factors at different levels of content have peak values. Upon combination of the comprehensive

analysis of significance, unconfined compressive strength measured the experiment, and cost, the optimal mix ratio of fluidic solidified soil with collapsible loess and red sandstone as aggregates is obtained as follows: the mass ratio of collapsible loess to red sandstone is 65:35, the cement content is 6%, the fly ash content is 15%, the lime content is 8%, and the NaOH content is 4%. The water-solid ratio satisfying the fluidity is 0.39 under this mix ratio. For the convenience of practical engineering applications, the total amount of materials other than water is calculated at 100%, and the proportion of factors A to E is 81.4%, 4.9%, 12.2%, 1%, and 0.5%, respectively.

The 28-day unconfined compressive strength of the fluidic solidified soil with the optimal mix ratio (denoted as S-S) was compared with that of the fluidic solidified soil with 6% cement (denoted as S-1), 6% cement, and 15% fly ash (denoted as S-2), and it was found that S-1 was 0.72 MPa and S-2 was 1.75 MPa. To achieve the same strength as S-S, a cement content of approximately 16% is required for S-1 (the unconfined compressive strength after 28 days with a single addition of 16% cement is 2.32 MPa). Upon comparison of S-2 with S-S, it can be seen that the unconfined compressive strength of the fluid solidified soil added with a small amount of lime and NaOH is more than 30% higher than that without the addition.

### 3.2 Establishment and Prediction of Regression Model

#### 3.2.1 Establishment of Regression Model

In order to better predict the unconfined compressive strength of fluidic solidified soil, a regression equation is established to provide a reference for the application design of fluidic solidified soil in engineering. The regression model for the mass ratio of collapsible loess to red sandstone, cement, fly ash, lime, and NaOH content is:

$$Y=a_1+b_1x_1+b_2x_2+b_3x_3+b_4x_4+b_5x_5+b_6x_1^2+b_7x_2^2+b_8x_3^2+b_9x_4^2+b_{10}x_5^2 \tag{1}$$

where  $Y$  is the unconfined compressive strength,  $x_1$  represents the mass ratio of collapsible loess to red sandstone,  $x_2$  represents cement content (%),  $x_3$  represents fly ash content (%),  $x_4$  represents lime content (%),  $x_5$  represents the content of NaOH (%),  $a_1$ ,  $b_1$ ,  $b_2$ ,  $b_3$ ,  $b_4$ ,  $b_5$ ,  $b_6$ ,  $b_7$ ,  $b_8$ ,  $b_9$ , and  $b_{10}$  are regression coefficients. According to the analysis of Table 7, the following regression equation can be obtained:

$$Y=-0.68+0.256x_1+0.375x_2+0.222x_3+0.151x_4+0.180x_5-0.031x_1^2 -0.028x_2^2 -0.019x_3^2 -0.018x_4^2-0.037x_5^2 \tag{2}$$

The corrected Chi-square value corresponding to the unconfined compressive strength is 0.0397, which means that the fitting model has a relatively good agreement with the observed data, so the regression equation is also effective and reliable.

#### 3.2.2 Validation of Regression Models

In order to check the accuracy of the regression equation, the predicted values of the regression equation were compared with the measured values. As can be seen from Figure 6, the predicted values are basically close to the measured values, with an

average residual value of 11.3%, which can fully meet the requirements for geotechnical testing.

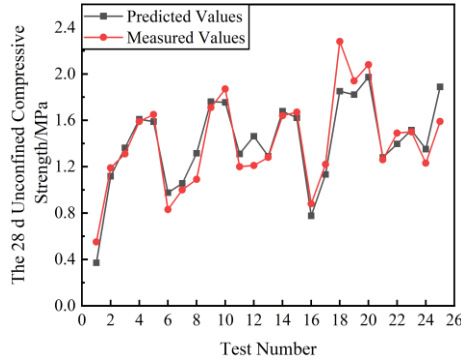


**Fig. 6.** Relationship between measured and predicted values of unconfined compressive strength

#### 4 Microstructure Analysis

At present, researchers generally use electron scanning microscopy (SEM) to observe the microstructure and morphology of materials to reveal the influence of microstructure on the strength formation of fluidic solidified soil. In order to better evaluate the feasibility of S-S, the microstructure of S-1 and S-2 at the same age (28 d) was compared with that of S-S, and the reasons for the strength formation of fluidic solidified soil at the microscopic level were evaluated by SEM. Its microscopic image is shown in Figure 7. Figure 7 shows the microstructure of each sample after being magnified by 2000 times.

As shown in Figure 7a, a small amount of aggregates (C-S-H) and needle substances (ettringite) are attached to the surface of the soil particles of S-1. The microstructure of the sample presents large voids, and the filling effect of the cementitious material generated between the loess and red sandstone particles is poor.

As depicted in Figure 7b, the voids in S-2 are significantly smaller than those in S-1, and the soil particles of S-2 are filled with substances such as C-S-H, C-A-H, CA-S-H, and unreacted fly ash particles. This is because fly ash is filled between soil particles, allowing the voids to be filled. In the absence of an activator, fly ash has lower activity and slower reaction, resulting in less C-A-H and CA-S-H generated, smaller agglomerate volume, and lower compactness.

As illustrated in Figure 7c, S-S forms dense large clumps of aggregates and needle-like substances. A large amount of these aggregates and substances are attached to the surface and voids of soil particles. As a result, the voids between the soil are basically filled by agglomerates. This is because the addition of alkali causes breakage of the Si-O and Al-O bonds of  $\text{SiO}_2$  and  $\text{Al}_2\text{O}_3$  in fly ash, generating a large amount of cementitious substances such as C-A-H and CA-S-H. These cementitious substances encapsulate the particles of collapsible loess and red sandstone, and fill the voids between soil particles, thereby making the microstructure of fluidic solidified soil denser, with

higher cementation ability, and greater unconfined compressive strength at the macro level.

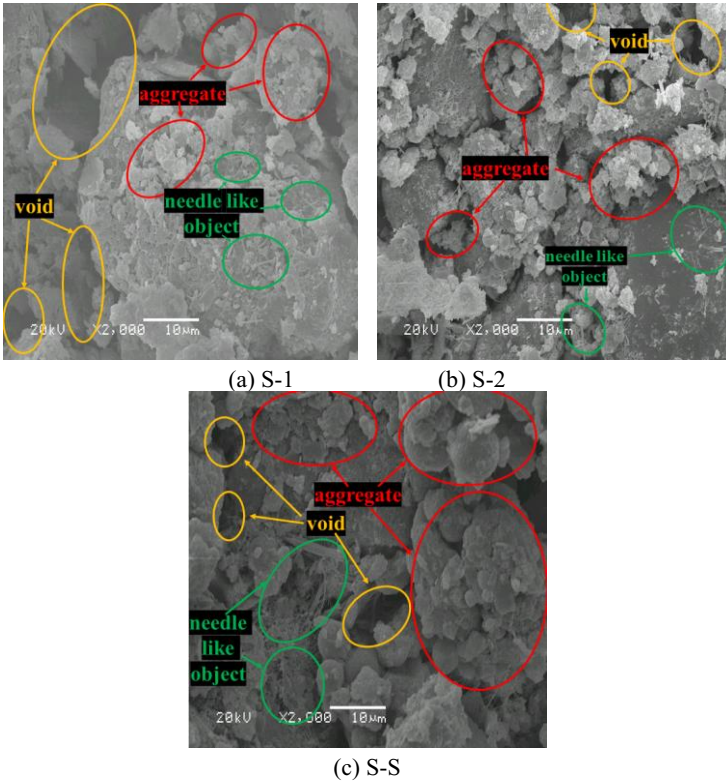


Fig. 7. Microstructure diagram

## 5 Conclusion

In this paper, the effects of the mass ratio of collapsible loess to red sandstone, cement, fly ash, lime, and NaOH content on the unconfined compressive strength of fluidic solidified soil are studied through orthogonal experiments. Furthermore, the microstructure of fluidic solidified soil with the optimal ratio is analysed. The following conclusions are drawn:

(1) The unconfined compressive strength of fluidic solidified soil increases with higher levels of cement, fly ash, and lime content. Conversely, the unconfined compressive strength initially rises and then declines with increasing mass ratio of collapsible loess to red sandstone and NaOH content. Overall, the order of influence on unconfined compressive strength is as follows: cement content > fly ash content > mass ratio of collapsible loess to red sandstone > NaOH content > lime content.

(2) The optimal mix ratio of fluidic solidified soil with collapsible loess and red sandstone as the aggregate is obtained as follows: the mass ratio of collapsible loess to

red sandstone is 65:35, the cement content is 6%, the fly ash content is 15%, the lime content is 8%, the NaOH content is 4%, and the water-solid ratio is 0.39.

(3) When the added aggregates are the same, the fluidic solidified soil with a single addition of cement requires an additional 10% cement to achieve the same strength as the optimal mix ratio. When other aggregates are the same, the 28 d unconfined compressive strength of the fluidic solidified soil under the optimal mix ratio is increased by more than 30% compared to the fluidic solidified soil without adding lime and NaOH. The optimal mix ratio not only optimizes material performance and improves construction efficiency, but also reduces costs and promotes sustainable development.

(4) A regression equation is proposed to predict the unconfined compressive strength of fluidic solidified soil with collapsible loess and red sandstone as aggregates, when there are changes in the material content, a more accurate prediction of the unconfined compressive strength can be achieved. The microscopic scanning results show that the compressive strength of fluidic solidified soil is determined by the sizes of internal voids and the amount of generated cementitious material.

(5) The fluidic solidified soil prepared with collapsible loess, red sandstone, cement, fly ash, lime, and NaOH not only effectively repurposes the engineering waste soil, but also has good compressive performance, making it feasible as engineering backfill material.

## Fund Project

General Project of National Natural Science Foundation of China (51978321); Changjiang Scholars and Innovation Team Support Program of Ministry of Education (IRT\_17R51).

## References

1. Ling T C, Kaliyavaradhan S K, Poon C S. (2018) Global perspective on application of controlled low-strength material (CLSM) for trench backfilling—An overview[J]. *Construction and Building Materials*, 158: 535-548. DOI: 10.1016/j.conbuildmat.2017.10.050.
2. Zhou B S, Jiang J, Chen Z B. (2016) Analysis of the technical benefits of "backfill compaction method in narrow area of foundation pit"[J]. *China Municipal Engineering*, (03): 93-95+99+128. DOI: 10.3969/j.issn.1004-4655.2016.03.028.
3. Nataraja M C, Nalanda Y. (2008) Performance of industrial by-products in controlled low-strength materials (CLSM)[J]. *Waste management*, 28(7): 1168-1181. <https://doi.org/10.1016/j.wasman.2007.03.030>.
4. Wang C, Li Y, Wen P, et al. (2023) A comprehensive review on mechanical properties of green controlled low strength materials[J]. *Construction and Building Materials*, 363: 129611. <https://doi.org/10.1016/j.conbuildmat.2022.129611>.
5. Li F, Liu C H, Wu Y B, et al. (2018) Influence of construction and demolished waste on controlled low strength material (CLSM)[J]. *Concrete*, (8): 71-73+78. DOI: 10.3969/j.issn.1002-3550.2018.08.017.

6. Zhang J, Wang J, Li X, et al. (2018) Rapid-hardening controlled low strength materials made of recycled fine aggregate from construction and demolition waste[J]. *Construction and Building materials*, 173: 81-89. <https://doi.org/10.1016/j.conbuildmat.2018.04.023>.
7. Zhou Y X, Wang J Z. (2019) Principle of ready-mixed solidified soil and its prospects for engineering application[J]. *New Building Materials*, 46(10): 117–120. DOI: 10.3969/j.issn.1001-702X.2019.10.027.
8. Liu X D. (2018) Application of Ready-mixed Fluid Stabilized Soil Technique in Foundation Trench Backfill Construction of Underground Comprehensive Pipe[J]. *Building Technology Development*, 45(04): 61-62. DOI: 10.3969/j.issn.1001-523X.2018.04.031.
9. CHEN R H, ZHEN P M. (2020) Analysis on Influencing Factors of Ready-mixed Fluid Solidified Soil based on Silty Clay[J]. *Chongqing Architecture*, 19(09): 32–36. DOI: 10.3969/j.issn.1671-9107.2020.09.32.
10. Wang Y, Yang H, Yang M M, (2022) et al. Preparation Tests of High Flowing Soil from Subway Residue Soil in Yellow River Flooding Area[J]. *Earth Science*, 47(12): 4698-4709. <https://doi.org/10.3799/dqkx.2022.186>.
11. Zhu J G, Wang J, Li X N, et al. (2023) Research on soil flow solidification of construction waste[J]. *Industrial Construction*, 53(S1): 695-697+728. <https://kns.cnki.net>.
12. Wang C C, Liu M Q, Song H Q, et al. (2023) Experimental Study on Properties of Red Mud, Steel Slag Powder and Cement Solidified Fluidized Soil[J]. *Bulletin of the Chinese Ceramic Society*, 42(07): 2488-2496. DOI: 10.16552/j.cnki.issn1001-1625.2023.07.006.
13. Satoh T, Tsuchida T, Mitsukuri K, et al. (2001) Field placing test of lightweight treated soil under seawater in Kumamoto port[J]. *Soils and Foundations*, 41(5): 145-154. [https://doi.org/10.3208/sandf.41.5\\_145](https://doi.org/10.3208/sandf.41.5_145).
14. Ministry of Housing and Urban-Rural Development of the People's Republic of China. (2011) Specification for Mix Proportion Design of Cement Soil: JGJ/T 233-2011[S]. Beijing: China Construction Industry Press. <https://www.mohurd.gov.cn/>.

**Open Access** This chapter is licensed under the terms of the Creative Commons Attribution-NonCommercial 4.0 International License (<http://creativecommons.org/licenses/by-nc/4.0/>), which permits any noncommercial use, sharing, adaptation, distribution and reproduction in any medium or format, as long as you give appropriate credit to the original author(s) and the source, provide a link to the Creative Commons license and indicate if changes were made.

The images or other third party material in this chapter are included in the chapter's Creative Commons license, unless indicated otherwise in a credit line to the material. If material is not included in the chapter's Creative Commons license and your intended use is not permitted by statutory regulation or exceeds the permitted use, you will need to obtain permission directly from the copyright holder.

